Inertial Properties in Haptic Devices: Non-Linear Inertia Shaping vs. Force Feedforward

Shamel Fahmi [*,**] **Thomas Hulin** [**]

[*] *Dynamic Legged Systems, Istituto Italiano di Tecnologia (IIT), Genova, Italy (e-mail: shamel.fahmi@iit.it)*
[**] *Institute of Robotics and Mechatronics, German Aerospace Center (DLR), Wessling, Germany (e-mail: thomas.hulin@dlr.de)*

Abstract: The inertia of haptic devices limits the user's manipulation and dynamically couples the Cartesian motion, which influences the transparency and fidelity in haptic feedback. By employing force-torque sensing, we investigate two approaches to reduce the apparent inertial effect of haptic devices and to overcome dynamic coupling. First, in order to shape the apparent inertia felt by the user, non-linear inertia shaping (NIS) is presented and introduced to the field of haptics. NIS is based on non-linear dynamic decoupling (NLD). Second, as a standard approach, force feedforward control (FF) is presented that uniformly scales down the apparent inertia. We demonstrate that FF is a special case of NIS, under the assumption that gravitational, centripetal and Coriolis terms are neglected. Simulations and experiments were conducted on DLR's bi-manual haptic device HUG. It is shown that NIS is suited to compensate for the coupling effects, while FF can reduce the apparent inertia more effectively.

Keywords: Feedback Linearization, Haptics and Haptic Interfaces, Force Control, Physical Human-Robot Interaction

1. INTRODUCTION

Haptics is advancing widely in diverse fields of research in robotics, especially human-robot interaction, telemanipulation, virtual manipulation, rehabilitation, etc. (Xia, 2016, Hannaford and Okamura, 2008, Hayward and Maclean, 2007). Commercial kinesthetic haptic devices are usually limited in their workspace, dynamic range and force/torque capabilities. One of the main trade-offs in haptic devices is between workspace and inertia of the device. A wider workspace usually comes along with a heavier manipulator that consequently results in higher inertia. In many applications, it is desirable to not perceive the inertial effects of the haptic device in order to provide fidelity to the user, which particularly becomes challenging for large workspaces (Gil et al., 2009). In the same context, commercial haptic devices are often designed as parallel mechanisms rather than serial manipulators due to the fact that parallel manipulators have higher accuracy and less dynamic inertia (Hayward and Maclean, 2007). However, parallel mechanisms are designed for manipulators with relatively smaller workspace. Likewise, due to its prior design, parallel mechanisms are usually manufactured with lower coupling effects compared to serial mechanisms (Zhang et al., 2006, Youcef-Touml and Asada, 1985).

When the inertia tensor of the haptic device is coupled, the motion of the device is also coupled. Thus, the motion of the end effector of the haptic device in a single direction will result in an undesired motion in the other directions. Such coupling effects were encountered by the authors during testings on their prototypical research device HUG (Hulin et al., 2011) and appeared to heavily disturb free-space movements, i.e. movements without displaying forces from a virtual environment.

One of the available solutions for the undesired effects of dynamical coupling and inertia in haptic devices is force feedforward control (FF), which is based on a force/torque sensor equipped in the haptic device (Hulin et al., 2015, Gil et al., 2009). FF results in scaling down all the dynamic effects including the inertia felt by the user as well as the coupling terms. In this paper, we propose using decoupling techniques (Albertos and Antonio, 2006, Khatib, 1987) as an alternative solution. The main two categories of decoupling are linear and non-linear decoupling. Linear decoupling techniques are suited for linear systems; such that when used on non-linear systems, the system has to be linearized and transfered into transfer function(s) or into a state space. Generally, linear decoupling is not always expedient especially when dealing with highly non-linear systems such as multi-degree-of-freedom (nDoF) robotic manipulators. The three main linear decoupling techniques that are widely used are feedback decoupling, dynamic decoupling and singular value decoupling (Albertos and Antonio, 2006). For non-linear systems, non-linear dynamic decoupling (NLD) may be used. NLD depends on estimating and compensating for the non-linear terms of the manipulator as well as the manipulator's mass matrix (Khatib, 1987). For the sake of clarity, it should be noted that NLD is widely known in the field of control theory as a special case of feedback linearization (Khalil, 1996).

In this paper, we propose implementing NLD to reduce the effects of dynamical coupling and high inertia for haptic devices. In the standard NLD approach, the decoupled system inertia is often set to identity. Thus, the system

Preprint submitted to 12th IFAC Symposium on Robot Control.
Received April 8, 2018.

behaves as a moving unit mass which is problematic in haptic feedback since the inertia of the haptic device contributes significantly to the stability of the feedback loop (Hulin et al., 2014). Thus, we consider augmenting the standard NLD approach with inertia shaping (IS). IS denotes imposing (regulating) the overall inertia of the rigid body. In haptics, IS implies modifying the apparent inertia felt by the user. Thus, by incorporating IS with NLD, the decoupled inertia is not identity. For instance, the apparent inertia could be shaped as a scale of the actual inertia or any other arbitrary shaped inertia. Such approach is crucial in haptics, because the operator needs to feel and sense the environment in a realistic manner. In other words, the user has to feel the inertia of the manipulated object rather than the inertia of the haptic device.

To the authors knowledge, IS using NLD is new in the field of haptics. Consequently, the main contributions of this paper are to extend the standard NLD approach with IS by assigning inertial properties to the haptic device, and to compare the suggested approach to the traditional FF approach. For the rest of this paper, NLD with IS will be referred to as non-linear inertia shaping (NIS). This paper is structured as follows. Section II describes NLD with IS for nDoF systems. Section III mentions FF (Hulin et al., 2015). In section IV, the experimental setup is introduced and simulation and experimental results are shown. Finally, the paper is concluded in section V.

2. NON-LINEAR INERTIA SHAPING

This section mentions the suggested NIS approach. First, NLD/feedback linearization is briefly summarized (Khatib, 1987, Khalil, 1996). Second, NIS is introduced by augmenting NLD in task space followed by the control law for trajectory tracking. Finally, the suggested approach is transformed from the end-effector into the coordinates of the handle grasped by the human operator.

2.1 Non-Linear Dynamic Decoupling

Consider the equation of motion of an nDoF manipulator expressed in the joint space

$$M_q(q)\ddot{q} + C_q(q,\dot{q}) + G_q(q) = \tau, \tag{1}$$

such that $M_q(q) \in \mathbb{R}^{n\times n}$ is the mass-matrix, $C_q(q,\dot{q}) \in \mathbb{R}^n$ is the centrifugal and Coriolis vector, and $G_q(q) \in \mathbb{R}^n$ is the vector for gravitational terms, all expressed in the joint space. Moreover, $q \in \mathbb{R}^n$ is the generalized coordinates vector of the nDoF manipulator and $\tau \in \mathbb{R}^n$ is the corresponding generalized torque vector for each joint. The equation of motion represented in (1) could be expressed in the task space coordinates as follows

$$M_x(q)\ddot{x} + C_x(q,\dot{q}) + G_x(q) = F, \tag{2}$$

such that $M_x(q) \in \mathbb{R}^{6\times 6}$ is the mass-matrix expressed in the task space, $C_x(q,\dot{q}) \in \mathbb{R}^6$ is the centrifugal and Coriolis vector expressed in the task space and $G_x(q) \in \mathbb{R}^6$ is the vector for gravitational terms expressed in the task space. Moreover, $x \in \mathbb{R}^6$ is the task space coordinates vector (end effector coordinates) of the nDoF manipulator and $F \in \mathbb{R}^6$ is the corresponding generalized force vector at the end effector. The relationship between the two equations of motion (1) and (2) are expressed as

$$\begin{aligned}
\dot{x} &= J(q)\dot{q},\\
F &= J^{\sharp T}(q)\tau,\\
M_x(q) &= J^{\sharp T}(q)M_q(q)J^{\sharp}(q),\\
C_x(q,\dot{q}) &= J^{\sharp T}(q)\left(C_q(q,\dot{q}) - M_q J^{\sharp}(q)\dot{J}(q)\dot{q}\right),\\
G_x &= J^{\sharp T}(q)G_q(q),
\end{aligned} \tag{3}$$

such that $J(q) \in \mathbb{R}^{6\times n}$ is the Jacobian matrix and $\dot{J}(q)$ is the first time derivative of the Jacobian matrix. For redundant manipulators, the Jacobian matrix is non-square and thus non-invertible. Thus, for the sake of generality, the pseudo-inverse of the Jacobian $J^{\sharp}(q)$ is used, which is expressed as

$$J^{\sharp}(q) = AJ^T(q)\left(J(q)AJ^T(q)\right)^{-1}, \tag{4}$$

such that A is a positive definite matrix. Without loss of generality, during simulations and experiments, A is chosen to be an identity matrix (i.e., the Moore-Penrose pseudo-inverse is used). Furthermore, the generalized forces expressed in the task space F are designed to be

$$F := \bar{F} + \hat{C}_x(q,\dot{q}) + \hat{G}_x(q), \tag{5}$$

such that $\hat{C}_x(q,\dot{q})$ and $\hat{G}_x(q)$ are estimates of the centripetal and Coriolis terms vector $C_x(q,\dot{q})$ and gravitational terms vector $G_x(q)$ respectively. Therefore, if ideal model estimates are assumed, (2) could be simplified to

$$M_x(q)\ddot{x} = \bar{F}, \tag{6}$$

such that $\bar{F} \in \mathbb{R}^{6\times n}$ is any control law for a gravity, centripetal and Coriolis compensated nDoF manipulator. Note that the resulted system is still a coupled system.

Consequently, if $\bar{F}$ is chosen as

$$\bar{F} := \hat{M}_x(q)I_{\mathrm{m}}^{-1}F_{\mathrm{E}}, \tag{7}$$

such that $\hat{M}_x(q)$ is an estimate of the mass-matrix $M_x(q)$ and $I_{\mathrm{m}} \in \mathbb{R}^{6\times 6}$ is an identity mass-matrix (diagonal mass-matrix of a unity mass at the diagonals). If ideal model estimates are assumed, (6) could be further simplified into

$$I_{\mathrm{m}}\ddot{x} = F_{\mathrm{E}}, \tag{8}$$

such that F_{E} implies any control law for a decoupled 6×1 DoF systems of unit mass.

2.2 Non-Linear Inertia Shaping

For the NIS approach, (7) should be redefined as

$$\bar{F} := \hat{M}_x(q)M_{x,\mathrm{des}}^{-1}(q)F_{\mathrm{E}}, \tag{9}$$

such that $M_{x,\mathrm{des}}(q) \in \mathbb{R}^{6\times 6}$ is the desired (shaped) inertia-matrix. $M_{x,\mathrm{des}}(q)$ is a positive definite non-singular dimensionless matrix. As a result, (8) becomes

$$M_{x,\mathrm{des}}(q)\ddot{x} = F_{\mathrm{E}}, \tag{10}$$

which corresponds to controlling a decoupled system of a desired inertia. The desired shaped inertia matrix $M_{x,\mathrm{des}}$ is perceived as the apparent inertia felt by the user. Ideally, it should represent the inertia of the virtual object being manipulated. However, in the real world, there is a lower limit for the scale-matrix due to stability issues, as it will be shown later in Sect. 4.

2.3 Control Law

If the control law is chosen for trajectory tracking of the end effector, the control input F_{E} could be expressed as

$$F_{\mathrm{E}} = M_{x,\mathrm{des}}(q)\ddot{x}_d + K_{\mathrm{v}}(\dot{x}_d - \dot{x}) + K_{\mathrm{p}}(x_d - x), \tag{11}$$

Preprint submitted to 12th IFAC Symposium on Robot Control.
Received April 8, 2018.

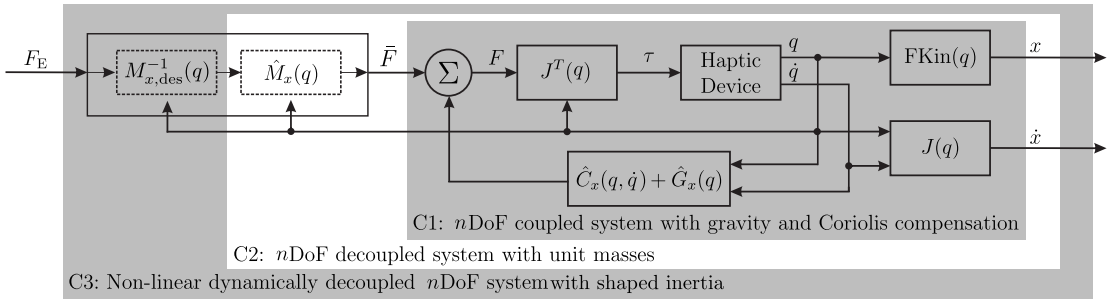

Fig. 1. Control architecture of NIS with three cascades (C1, C2 and C3)

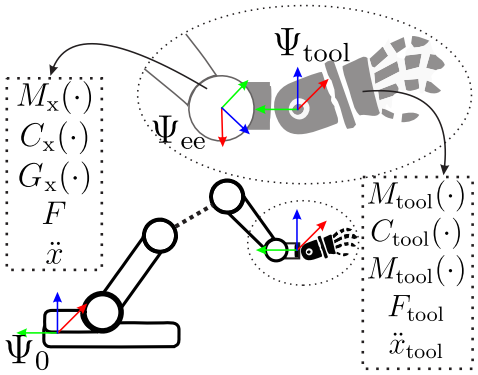

Fig. 2. nDoF manipulator: system dynamics expressed in the end effector frame Ψ_{ee} and in the tool frame Ψ_{tool}

such that $\ddot{x}_d$, $\dot{x}_d$ and x_d are the desired position, velocity and acceleration of the end effector respectively. Moreover, the diagonal gains K_{p} and K_{v} are the corresponding proportional and derivative action for each task coordinate. As a result, the behavior of the closed loop of the system with ideal model estimates is expressed as

$$M_{x,\mathrm{des}}(q)\ddot{e} + K_{\mathrm{v}}\dot{e} + K_{\mathrm{p}}e = 0, \tag{12}$$

such that $e = x_d - x$ is the tracking error of the end effector position. However, in the real world, obtaining ideal model estimates for $M_x(q)$, $C_x(q,\dot{q})$ and $G_x(q)$ is not possible. Thus, the equation of motion of the non-linear decoupled system (10) is expressed as

$$\begin{aligned}\ddot{x} = M_x^{-1}(\cdot)\hat{M}_x(\cdot)M^{-1}_{x,\mathrm{des}}(\cdot)F_{\mathrm{E}} + \\ M_x^{-1}(\cdot)[(\hat{C}_x(\cdot) - C_x(\cdot)) + (\hat{G}_x(\cdot) - G_x(\cdot))],\end{aligned} \tag{13}$$

such that the difference between the actual and the estimated matrices/vectors are considered as disturbances Δ that are compensated in the trajectory tracking such that the closed loop behavior of the system with non-ideal model estimates is expressed as

$$M_{x,\mathrm{des}}(q)\ddot{e} + K_{\mathrm{v}}\dot{e} + K_{\mathrm{p}}e + \Delta = 0. \tag{14}$$

Fig. 1 represents the suggested NIS approach in which the control architecture is divided into three subsystems. In subsystem C1, the haptic device is compensated for gravitational, centripetal and Coriolis terms at the task space. It is important to note that the gravity compensation should be compensated in the joint space G_q rather than the task space G_x especially for redundant manipulators, because if the compensation is for G_x, the redundant joints in null space are not gravity compensated. Moreover, C2 represents the standard NLD approach with unit masses while C3 represents the entire NIS approach.

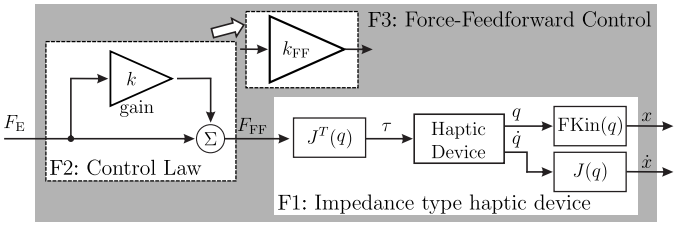

Fig. 3. Control architecture of FF for impedance type haptic devices.

2.4 System Dynamics in the Tool Frame

In haptic interaction, the human usually grasps a tool attached to the end effector of the manipulator. Thus, with the assumption of a tool with a body-fixed frame Ψ_{tool} at its center of gravity attached to the haptic device (see Fig. 2), the system dynamics $M_x(\cdot)$, $C_x(\cdot)$, $G_x(\cdot)$ and F of the manipulator expressed in the end effector frame Ψ_{ee} could be transformed into the tool frame Ψ_{tool} with

$$\begin{aligned}M_{\mathrm{tool}}(\cdot) &= A_{d_{H_{\mathrm{tool}}}}^{T} \quad M_x(\cdot) \quad A_{d_{H_{\mathrm{tool}}}}, \\ C_{\mathrm{tool}}(\cdot) &= A_{d_{H_{\mathrm{tool}}}}^{-T} \quad C_x(\cdot), \\ G_{\mathrm{tool}}(\cdot) &= A_{d_{H_{\mathrm{tool}}}}^{-T} \quad G_x(\cdot), \\ F_{\mathrm{tool}} &= A_{d_{H_{\mathrm{tool}}}}^{-T} \quad F,\end{aligned} \tag{15}$$

such that

$$A_{d_{H_{\mathrm{tool}}}} := \begin{bmatrix} R & \tilde{p}R \\ 0 & R \end{bmatrix}, \tag{16}$$

is the adjoint of the tool frame relative to the end effector of the manipulator (Murray et al., 1994). Henceforth, R is the relative rotation matrix between the end effector frame Ψ_{ee} and the tool frame Ψ_{tool}. Moreover, $\tilde{p}$ is the skew symmetric matrix of the relative position between the end effector frame and the tool frame. If the attached tool has significant inertia and dynamics, then the total system dynamics are simply the summation of the dynamics of the manipulator and the tool (Khatib, 1988).

Finally, the equation of motion of the manipulator expressed in the tool frame can be written as

$$M_{\mathrm{tool}}(q)\ddot{x}_{\mathrm{tool}} + C_{\mathrm{tool}}(q,\dot{q}) + G_{\mathrm{tool}}(q) = F_{\mathrm{tool}}. \tag{17}$$

3. FORCE FEEDFORWARD CONTROL

One of the traditional techniques that are used in haptics to tackle the coupling and inertia effects is FF. FF has been validated on robotic systems such as the LHIfAM (Gil et al., 2009), the German Aerospace Center (DLR) bi-manual haptic device HUG (Hulin et al., 2011, Hulin et al., 2015) and the sigma.7 (Tobergte et al., 2011). The

Preprint submitted to 12th IFAC Symposium on Robot Control.
Received April 8, 2018.

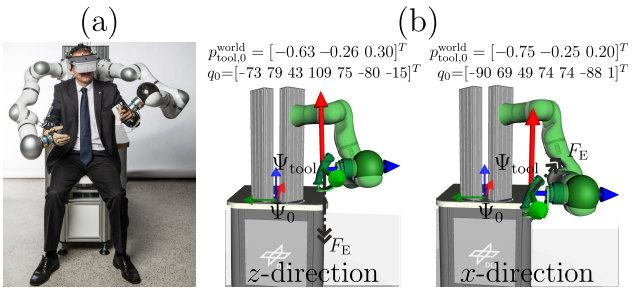

Fig. 4. (a) The DLR bi-manual haptic device and (b) its simulator. The two main frames are the world frame Ψ_0 and the tool frame Ψ_{tool}. Each frame is indicated by its corresponding three axes (x, y and z axes are represented by red, green and blue arrows respectively). The initial translation conditions $p^{\text{world}}_{\text{tool},0}$ and initial joints q_0 are also shown.

main idea of FF is that it scales down the dynamic effects including the inertia and coupling effects of the haptic device that is felt by the operator. This is achieved by artificially scaling up the force that is operated by the user's movements with a gain of k_{FF} using a force/torque sensor that is equipped in these haptic devices. FF does not decouple the system but only uniformly reduces the dynamic effects of the manipulator. The control law $F_{\text{tool,FF}}$ for the manipulator's equations of motion (17) using FF is defined as

$$F_{\text{tool,FF}} := k_{\text{FF}} F_{\text{E}}, \tag{18}$$

such that the force feedforward gain k_{FF} is defined as

$$k_{\text{FF}} := 1 + k, \tag{19}$$

as shown in Fig. 3 which represents the control architecture of FF for haptic devices of impedance type. Finally, it should be noted that FF may be considered a special case of NIS, in which the compensation for gravitational, centripetal and Coriolis terms are neglected and the desired inertia matrix is denoted as $M_{x,\text{des}}(q) = \frac{1}{k_{\text{FF}}} \hat{M}_x(q)$. For more information regarding FF for haptic devices, the reader is referred to Hulin et al., 2015.

4. EXPERIMENTS

This section discusses the conducted simulations and experiments; and the obtained results. Firstly, the experimental setup is described. Secondly, the experimental procedures are explained followed by the definitions of the coupling ratios. Finally, the results are represented and discussed.

4.1 Experimental Setup

In this context, the haptic device that is used to conduct simulations and experiments is HUG (Hulin et al., 2011), which is equipped with two DLR/KUKA light weight robots (LWR). The LWR is a 7 DoF serial manipulator with torque and position sensors at each joint to permit admittance and impedance control. A magnetic safety clutch is added to each of the end effectors for the human to grasp (see Fig. 4a). The haptic device is equipped with null-space optimization, singularity avoidance as well as collision avoidance between the two robots and the robots with the base. The workspace of HUG is optimized to fit the workspace of the human arm such that the operator can naturally perform tasks with minimal limitations by the haptic device. Finally, an interactive HUG-simulator has been implemented at DLR such that the same parameters of HUG are represented which made it possible to simulate any developed control techniques on HUG offline without operating the actual haptic device.

4.2 Experimental Procedure

In simulations and experiments, only the left robot was used (the operator's left and the reader's right as shown in Fig. 4). Simulations and experiments were conducted to evaluate the effect of decoupling and inertia shaping for HUG using NIS and FF. The experiments were conducted on both HUG-simulator and HUG. To evaluate the coupling effects, a force was applied at the tool in to move in one direction only while investigating the motion due to coupling in other directions and orientations. Ideally, the decoupled manipulator should maneuver in the direction of the driven force without any motion in other directions and orientations. Therefore, a real weight of 0.5 kg hung at the tool tip was suggested. However, due to the suspension of the weight, the desired force in a single direction was not feasible. Additionally, the suspended weight was only feasible in the z-direction (i.e. along the gravity vector). Thus, other directions would not have been investigated using the weight. Consequently, a "virtual" force of 5 N was given as an input to the haptic device. Utilizing the virtual force allowed restricting the driven force to one direction in all possible directions and, in addition, led to a better repeatability.

Two scenarios were conducted under the same conditions with different directions of the force (indicated by F_{E} in Fig. 4b). In the first scenario, the virtual force was pointing downwards (negative z-axis of the world frame) while in the second scenario, the virtual force was pointing into the paper (positive x-axis of the world frame). Furthermore, The translation and orientation of the tool frame Ψ_{tool} were recorded. To evaluate the coupling effects, coupling ratios for translations $\eta_{\perp i}$ and orientations η_φ are defined as

$$\eta_{\perp i} := \frac{\int_{i_0}^{i_f} \varepsilon_{\perp i,\text{NIS}}(i)di}{\int_{i_0}^{i_f} \varepsilon_{\perp i,\text{FF}}(i)di},$$
$$\eta_\varphi := \frac{\int_{i_0}^{i_f} \varepsilon_{\varphi,\text{NIS}}(i)di}{\int_{i_0}^{i_f} \varepsilon_{\varphi,\text{FF}}(i)di}, \tag{20}$$

such that $\eta_{\perp i}$ represents the coupling effects due to the translation in the ith direction. The symbol $\perp i$ denotes the two corresponding orthogonal axes of the axis i. Moreover, η_φ represents coupling effects in orientation due to the translation in the coordinate axis i. The terms $\varepsilon_{\perp i,\text{NIS}}(i)$ and $\varepsilon_{\perp i,\text{FF}}(i)$ represent the Euclidean norm of the error (with respect to the initial conditions) of the two orthogonal axes of the coordinate i in NIS and FF respectively. Furthermore, $\varepsilon_{\varphi,\text{NIS}}(i)$ and $\varepsilon_{\varphi,\text{FF}}(i)$ represent the absolute error of the angle φ (the angle of the orientation using axis-angle representation with respect to the initial condition $\varphi(i_0)$) in NIS and FF respectively.

In this context, three FF gains were selected ($k_{\text{FF}} = 1, 2, 3$). FF gain of 1 implies no FF control while FF

Preprint submitted to 12th IFAC Symposium on Robot Control.
Received April 8, 2018.

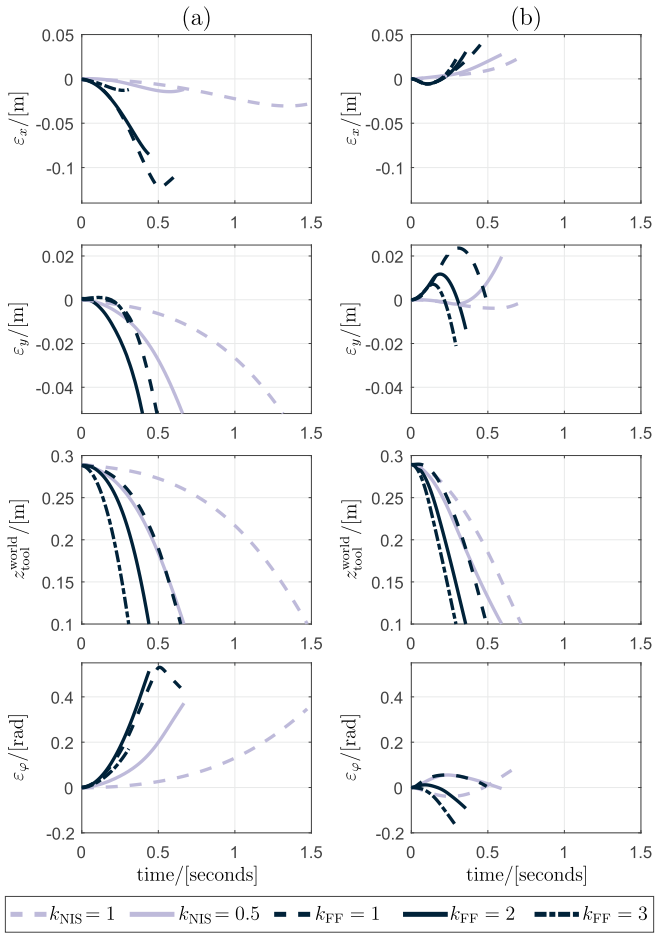

Fig. 5. Scenario 1: virtual force in the z-direction relative to the world frame Ψ_0. The plot includes tracking errors ε_x and ε_y, translation in z and angle φ in both (a) experiments and (b) simulations.

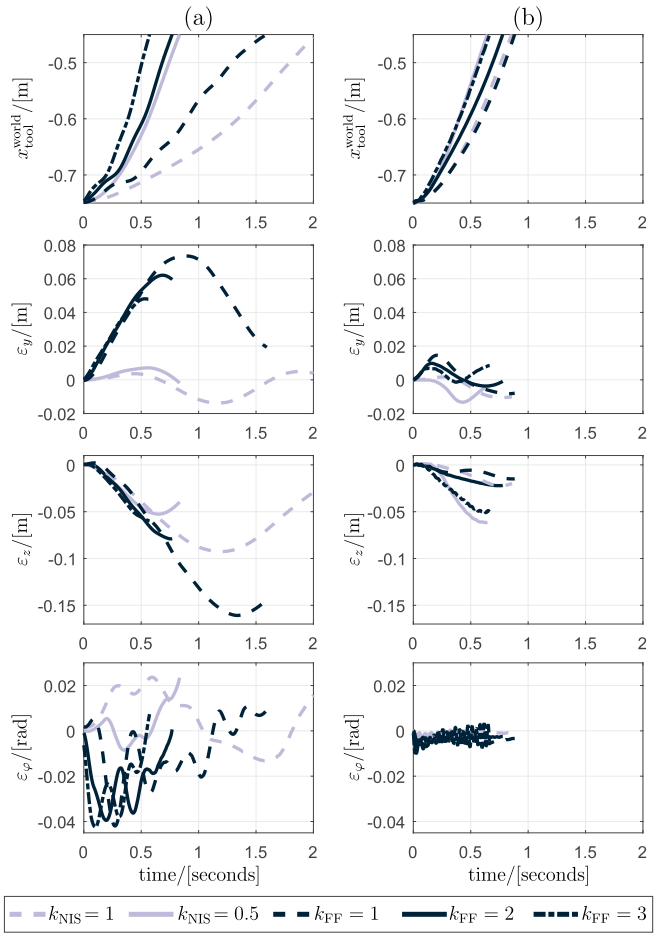

Fig. 6. Scenario 2: virtual force in the x-direction relative to the world frame Ψ_0. The plot includes tracking errors ε_y and ε_z, translation in x and angle φ in both (a) experiments and (b) simulations.

gain of 3 implies a reduction of inertia up to 33%. It was experimentally proven that with a FF gain of more than 3 the system was unstable. Furthermore, the desired inertia $M_{x,\text{des}}(q)$ was chosen to be the diagonal matrix of the estimated mass matrix represented in the tool frame $\hat{M}_{\text{tool}}(q)$ pre-multiplied by the scalar gain k_{NIS}. Note that k_{NIS} and k_{FF} are reciprocals hence, $k_{\text{FF}} = 1, 2, 3$ correspond to $k_{\text{NIS}} = 1, 0.5, 0.333$. However, NIS gains of $k_{\text{NIS}} = 1, 0.5$ are only chosen since lower gains of NIS drove the system unstable.

4.3 Results

The two scenarios were conducted on HUG-simulator and HUG while recording the 3 coordinates of translation $p_{\text{tool}}^{\text{world}}$ and the angle φ resulting in 16 plots. Each plot shows five curves for $k_{\text{NIS}} = 0.5, 1$ and $k_{\text{FF}} = 1, 2, 3$. Fig. 5 represents the experiments (Fig. 5a) and simulations (Fig. 5b) with an initial position of the tool with respect to the world frame of $p_{\text{tool},0}^{\text{world}} = [-0.63, -0.26, 0.29]^T$ and a final condition of $z_f = 0.1$. Moreover, Fig. 6 represents the experiments (Fig. 6a) and simulations (Fig. 6b) with an initial position of the tool with respect to the world frame of $p_{\text{tool},0}^{\text{world}} = [-0.75, -0.25, 0.2]^T$ and a final condition of $x_f = 0.45$. The initial conditions were chosen to avoid any other influences resulting from null-space optimization or joint limits prevention that are equipped in HUG. Note that the robot is closer to reaching the joint limits in the first scenario rather than in the second one. Finally, Table I provides the obtained coupling ratios in translation and rotation for each of the two scenarios.

Table 1. Coupling ratios in the two scenarios

k_{NIS}	k_{FF}	Parameter	z-direction	x-direction
1	1	$\int_{i_0}^{i_f} \varepsilon_{\perp i,\text{NIS}}(i)di$	0.0157	0.0373
		$\int_{i_0}^{i_f} \varepsilon_{\perp i,\text{FF}}(i)di$	0.0384	0.0701
		$\eta_{\perp i}$	0.4089	0.5320
		$\int_{i_0}^{i_f} \varepsilon_{\varphi,\text{NIS}}(i)di$	0.0646	0.0063
		$\int_{i_0}^{i_f} \varepsilon_{\varphi,\text{FF}}(i)di$	0.1501	0.0075
		η_{φ}	0.4304	0.8395
0.5	2	$\int_{i_0}^{i_f} \varepsilon_{\perp i,\text{NIS}}(i)di$	0.0104	0.0242
		$\int_{i_0}^{i_f} \varepsilon_{\perp i,\text{FF}}(i)di$	0.0242	0.0416
		$\eta_{\perp i}$	0.4298	0.5810
		$\int_{i_0}^{i_f} \varepsilon_{\varphi,\text{NIS}}(i)di$	0.0691	0.0045
		$\int_{i_0}^{i_f} \varepsilon_{\varphi,\text{FF}}(i)di$	0.1107	0.0120
		η_{φ}	0.6245	0.3774

As shown in Fig. 5, Fig. 6 and Table I, FF is generally faster than NIS because decoupling the system results in a more constrained motion. Additionally, the coupling ratios $\eta_{\perp i}$ and $\eta_{\perp \varphi}$ in the two scenarios are smaller than one,

Preprint submitted to 12th IFAC Symposium on Robot Control.
Received April 8, 2018.

which implies that NIS is better in dealing with coupling effects than FF both in translation and rotation. It is also shown that the higher the FF gain k_{FF} or the lower the NIS gain k_{NIS}, the better the system is in dealing with coupling effects and the faster the system is (due to the fact that the value of the compensated inertia is higher thus less inertia is felt by the operator). However, the effect of the gains k_{FF} and k_{NIS} were negligible in the rotation in the x-direction and z-direction respectively. Finally, the error in the rotation in the first scenario is greater than in the second one due to the fact that in the first scenario, the robot is close to joint limits. Thus the influence of null-space optimization becomes apparent which causes further rotations.

5. CONCLUSIONS

This paper presented a novel approach to shape the apparent inertia of haptic devices and to overcome dynamic coupling by introducing NIS. NIS was compared to FF as a standard approach in haptics that uniformly scales down inertia. The relationship between NIS and FF was presented, in which we demonstrated that the latter is a special case of the former method, when gravitational, centripetal and Coriolis terms are neglected. It has been shown that both NIS and FF resulted in a reduction in the inertia felt by the user as well as in the coupling terms. NIS decoupled the dynamics more effectively than FF while FF reduced the inertia more significantly compared to NIS. In particular, FF can reduce the inertia felt by the user up to 33% while NIS can reduce the inertia up to 50%.

Haptic interaction systems are closed loop systems that include the haptic device, human operator and the interacting environment. Consequently, stability of the haptic device and the haptic system is crucial while still maintaining fidelity and transparency for the operator which are usually contradicting. Henceforth, several research approaches investigated stability and passivity for haptic interaction systems and employed stability and passivity controllers for such systems (Hulin et al., 2014, Colgate and Schenkel, 1994). However, these analyses were usually investigated for systems with 1 DoF which is therefore limited to specific cases. In fact, Che et al. (2016) stated the importance of extending these analysis for nDoF systems. As a result, for the future work, since NIS decouples system dynamics, this paper may be a step towards investigating the 1 DoF approaches that study passivity and stability of haptic interaction for higher DoFs. However, one has to keep in mind that the NIS itself affects the stability reserve of the haptic system. This paper does not analyze or investigate stability for non-linear nDoF systems. However, this paper fits perfectly into moving a step towards such analysis. Moreover, user studies would reveal which of the two approaches leads to a more realistic impression of virtual world simulation. Finally, the suggested NIS approach can equally be applied to telemanipulation systems in order to decouple the combined dynamics between the master-slave system.

REFERENCES

Albertos, P. and Antonio, S. (2006). *Multivariable control systems: an engineering approach*. Springer Science & Business Media.

Che, Y., Haro, G.M., and Okamura, A.M. (2016). Two is not always better than one: Effects of teleoperation and haptic coupling. In *2016 6th IEEE International Conference on Biomedical Robotics and Biomechatronics (BioRob)*, 1290–1295.

Colgate, J.E. and Schenkel, G. (1994). Passivity of a class of sampled-data systems: application to haptic interfaces. In *American Control Conference, 1994*, volume 3, 3236–3240 vol.3.

Gil, J.J., Rubio, A., and Savall, J. (2009). Decreasing the apparent inertia of an impedance haptic device by using force feedforward. 17(4), 833–838.

Hannaford, B. and Okamura, A.M. (2008). *Haptics*, 719–739. Springer Berlin Heidelberg, Berlin, Heidelberg.

Hayward, V. and Maclean, K.E. (2007). Do it yourself haptics: part I. *IEEE Robotics Automation Magazine*, 14(4), 88–104.

Hulin, T., Albu-Schäffer, A., and Hirzinger, G. (2014). Passivity and stability boundaries for haptic systems with time delay. *IEEE Transactions on Control Systems Technology*, 22(4), 1297–1309.

Hulin, T., Hertkorn, K., Kremer, P., Schätzle, S., Artigas, J., Sagardia, M., Zacharias, F., and Preusche, C. (2011). The DLR bimanual haptic device with optimized workspace. In *2011 IEEE International Conference on Robotics and Automation*, 3441–3442.

Hulin, T., Alessandro, C., Vodermayer, B., and Riener, R. (2015). Evaluation of force feedforward control for actuators with limited dynamics and time delay. *STAMAS Workshop - Smart technology for artificial muscle applications in space, Madrid, Spain*.

Khalil, H.K. (1996). Nonlinear systems. *Prentice-Hall, New Jersey*.

Khatib, O. (1987). A unified approach for motion and force control of robot manipulators: The operational space formulation. *IEEE Journal on Robotics and Automation*, 3(1), 43–53.

Khatib, O. (1988). Object manipulation in a multi-effector robot system. In *Proceedings of the 4th international symposium on Robotics Research*, 137–144. MIT Press.

Murray, R.M., Li, Z., and Sastry, S.S. (1994). *A Mathematical Introduction to Robotic Manipulation*. CRC Press.

Tobergte, A., Helmer, P., Hagn, U., Rouiller, P., Thielmann, S., Grange, S., Albu-Schäffer, A., Conti, F., and Hirzinger, G. (2011). The sigma.7 haptic interface for mirosurge: A new bi-manual surgical console. In *2011 IEEE/RSJ International Conference on Intelligent Robots and Systems*, 3023–3030.

Xia, P. (2016). Haptics for product design and manufacturing simulation. *IEEE Transactions on Haptics*, 9(3), 358–375.

Youcef-Touml, K. and Asada, H. (1985). Dynamic decoupling and control of a direct-drive manipulator. In *1985 24th IEEE Conference on Decision and Control*, 2052–2058.

Zhang, J., Li, W., Wang, X., and Gao, F. (2006). Study on kinematics decoupling for parallel manipulator with perpendicular structures. In *IEEE/RSJ International Conference on Intelligent Robots and Systems*, 748–753.

Preprint submitted to 12th IFAC Symposium on Robot Control.
Received April 8, 2018.